AIP | Applied Physics Letters

Theory of plasmonic near-field enhanced absorption in solar cells

N. Lagos, M. M. Sigalas, and E. Lidorikis

Citation: Appl. Phys. Lett. **99**, 063304 (2011); doi: 10.1063/1.3623759
View online: http://dx.doi.org/10.1063/1.3623759
View Table of Contents: http://apl.aip.org/resource/1/APPLAB/v99/i6
Published by the American Institute of Physics.

Theory of plasmonic near-field enhanced absorption in solar cells

N. Lagos,[1,2] M. M. Sigalas,[2] and E. Lidorikis[3,a)]
[1]*Institute of Materials Science, N.C.S.R "Demokritos, Agia Paraskevi, Athens 15310, Greece*
[2]*Department of Materials Science, University of Patras, Patras 26504, Greece*
[3]*Department of Materials Science & Engineering, University of Ioannina, Ioannina 45110, Greece*

(Received 7 June 2011; accepted 16 July 2011; published online 11 August 2011)

We derive analytical expressions for the absorption enhancement expected when dilute suspensions of small metallic nanoparticles are inserted inside an organic semiconductor. A comparison with accurate numerical simulations shows excellent agreement for a wide range of volume filling ratios and even in the case of mixing different types of metals. These results are invaluable tools in optimizing the absorption performance of plasmonic thin-film organic solar cells. © *2011 American Institute of Physics*. [doi:10.1063/1.3623759]

Organic solar cells[1] hold promise for renewable energy because of their low cost, flexibility, and light weight. On the flip-side, they suffer from short carrier diffusion lengths, of the order of few tens of nanometers,[1] placing restrictions on the active layer thickness. For thin devices, light absorption is reduced and techniques to improve it are needed. Plasmonics have emerged as a promising approach for doing that in both organic and inorganic solar cells.[2] This includes metallic scattering elements on the surface,[3–9] back[10,11] or inside the semiconductor[12–15] in order to scatter and trap the incident light[3–5,10,11] and/or enhance the absorption due the enhanced near fields around the scattering elements.[6–9,12–15]

Noble metal nanoparticles (MNP) have been typically utilized due to their surface plasmon resonance (SPR). Measurements[3,6–8] have shown significant improvements in organic solar cell efficiencies after incorporating MNPs, becoming almost doubled in some experiments.[6] It is important that the MNP benefit is strong enough so that it is not countered by absorption inside the MNPs or by carrier recombination at the MNP surface.[14] Generally, the SPR-mediated absorption enhancement (AE) is significant when the semiconductor's intrinsic absorption is small.[16] The need to establish good design principles necessitates a simple and intuitive understanding of the AE the MNPs can achieve. Despite progress in this field, there is still no simple analytical solution to this. Here, we study the AE stemming from the enhanced near-fields of small MNPs dispersed inside an organic solar cell and derive close-form analytical expressions. We simplify the problem with three approximations: (1) point dipole limit,[17] (2) low intrinsic semiconductor absorption (absorption proportional to local intensity), (3) simple geometry without interfaces and standing waves. While approximation (3) is far from a realistic device, it will allow us nevertheless to extract useful relations that can improve our understanding and intuition, which may be then transferable to practical device geometries.

A spherical MNP of radius a in a host of dielectric constant ε_h, is irradiated by a plane wave of amplitude E_0, frequency ω and polarization $\hat{\mathbf{x}}$, shown in Fig. 1(a). The incident field excites an electric dipole at the MNP center

$$\mathbf{p} = \varepsilon_0 \varepsilon_h \alpha_{np}(\omega)\mathbf{E} \approx \varepsilon_0 \varepsilon_h \alpha_{np}(\omega) E_0 \hat{\mathbf{x}}, \tag{1}$$

where the local field $\mathbf{E}$ at the MNP is approximately the same as the incident (a $e^{-i\omega t}$ dependence is assumed for $\mathbf{p}$, $\mathbf{E}$). The sphere polarizability α_{np} in the Mie theory[18] is

$$\alpha_{np}(\omega) = \frac{6\pi i}{k^3} \frac{\tilde{m}\psi_1(\tilde{m}ka)\psi_1'(ka) - \psi_1(ka)\psi_1'(\tilde{m}ka)}{\tilde{m}\psi_1(\tilde{m}ka)\xi_1'(ka) - \xi_1(ka)\psi_1'(\tilde{m}ka)}, \tag{2}$$

where ψ_1, ξ_1 are Riccati-Bessel functions, $k = n_h\omega/c$, and $\tilde{m} \equiv \tilde{m}(\omega) = \tilde{n}_p(\omega)/n_h$, where $\tilde{n}_p(\omega) = \sqrt{\tilde{\varepsilon}_p(\omega)}$ and $n_h = \sqrt{\varepsilon_h}$ are the MNP's and host's indices of refraction. For $a \ll \lambda$, Eq. (2) simplifies to[18]

$$\alpha_{np}(\omega) \approx 4\pi a^3 (\tilde{\varepsilon}_p(\omega) - \varepsilon_h)/(\tilde{\varepsilon}_p(\omega) + 2\varepsilon_h). \tag{3}$$

MNP's index differs from the bulk value due to a reduced free electron relaxation caused by surface scattering.[19] To account for this, we first assume a Drude-Lorentz model

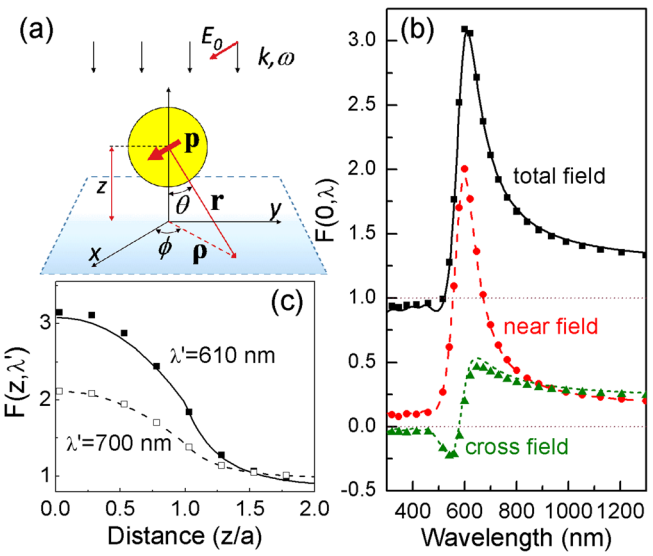

FIG. 1. (Color online) (a) Schematic of the geometry considered. (b) Comparison between Eq. (9) (lines) and accurate FDTD simulations (symbols), for a square array of $a = 4$ nm Au MNPs in a $n_h = 2$ host at periodicity $L = 21.5$ nm ($f = 2.7\%$). The enhancement is calculated on a plane going through the nanoparticle center ($z = 0$). Total, near, and cross field contributions are shown. (c) Total enhancement vs z at $\lambda = 610$ nm (peak enhancement) and $\lambda = 700$ nm.

a)Electronic mail: elidorik@cc.uoi.gr.

$$\tilde{\varepsilon}_p(\omega) = \varepsilon_\infty - \frac{\omega_p^2}{\omega^2 + i\omega/\tau} + \sum_{j=1}^{N} \frac{\Delta\varepsilon_j \Omega_j^2}{\Omega_j^2 - \omega^2 - i\omega\Gamma_j}, \quad (4)$$

where all parameters are adjusted to reproduce the experimental bulk metallic dielectric function[17] and then rescale the free electron relaxation time according to $\tau^{-1} \to \tau^{-1} + v_F/a$, where v_F is the Fermi velocity.

Furthermore since we will assume arrays of MNPs at some finite volume filling ratio (say a cubic array of side L), the MNP local field is affected by the fields scattered from other MNPs. This is done within the Clausius-Mossotti theory[20]

$$\alpha_{np} \to \alpha_{np}/(1 - N\alpha_{np}/3) \Rightarrow Q \to Q/(1 - f \cdot Q), \quad (5)$$

where N is the MNP number density, $f = 4\pi a^3/3L^3$ is their volume filling ratio, and Q the normalized polarizability $Q(\omega) = \alpha_{np}(\omega)/(4\pi a^3)$. Finally, the incident power is effectively reduced by absorption inside the MNPs. For $a \ll \lambda$, Mie theory[18] gives the absorption cross section $C_{abs} = 4\pi a^3 k \mathrm{Im}\{Q\}$. We crudely take this effect into account by rescaling the incident intensity

$$|E_0|^2 \to |E_0'|^2 = |E_0|^2(1 - C_{abs}/L^2) = \gamma|E_0|^2. \quad (6)$$

The total field at $\mathbf{r}$ on a horizontal plane at distance z from the nanoparticle center is[20]

$$\mathbf{E}(\mathbf{r},\omega) \approx E_0' e^{ikr\cos\theta}\hat{\mathbf{x}} + e^{ikr}(4\pi\varepsilon_0\varepsilon_h)^{-1} \times \left[k^2 r^{-1}\hat{\mathbf{r}} \times (\mathbf{p} \times \hat{\mathbf{r}}) + (r^{-3} - ikr^{-2})[3\hat{\mathbf{r}}(\hat{\mathbf{r}} \cdot \mathbf{p}) - \mathbf{p}]\right]. \quad (7)$$

The first term in the square bracket is the dipole radiation field while second and third are the dipole near-fields. At resonance, they exceed the incident field and drive the AE. These three terms scale with distance and wavelength as $\propto \lambda^{-2} r^{-1}$ and $\propto r^{-3}$, $\propto \lambda^{-1} r^{-2}$, respectively. The $\propto r^{-3}$ term dominates for particles and distances small compared to the wavelength. In the following, we only consider the near-field and generally ignore the dipole radiation term (except for its cross term with r^{-3} which yields a $\propto r^{-2}$ contribution).

The absorption is $A(\mathbf{r},\omega) = 1/2\mathrm{Re}\{\Sigma(\omega)\}\ |E(\mathbf{r},\omega)|^2$, with $\Sigma(\omega)$ the optical conductivity. Normalizing by the absorption without MNPs and using Eq. (7), the AE is

$$F(\mathbf{r},\omega) = \gamma\Big\{1 + a^6|Q|^2 r^{-6}\left[3x^2 + 1 + k^2r^2(5x^2 - 1)\right] + 2a^3|Q|r^{-3}\left[(3x^2 - 1)\cos\Delta + kr(3x^2 - 1)\sin\Delta\right]\Big\} \quad (8)$$

where $x = \sin\theta\cos\phi$, $\Delta = kr - kz + \zeta$ and $Q = |Q|e^{i\zeta}$. The first term is from the incident wave, the second from the MNP near-fields, and the last from the cross term between incident and MNP near-field. We stress that Eq. (8) assumes a perturbative effect of the absorption, i.e., it is small everywhere so that fields are well estimated by Eq. (7). Our approach, thus, applies better for weakly absorbing materials, which is anyway where the AE is more critical. We should also note, however, the general rule that the semiconductor's absorption rate must exceed the plasmon decay rate, otherwise, the absorbed energy may dissipate into ohmic damping in the MNP.[2]

We perform spatial integration first on a plane at distance z from the MNP (see Fig. 1) and then vertically. This is convenient if we need the AE within planar regions of finite thickness.[6–8] For particles arranged in a cubic lattice of side L the planar enhancement is normalized by L^2. Integration over the area outside the MNP puts a lower limit $r_{\min} = |z|/\delta$, with $\delta = \min(1, |z|/a)$. The planar AE is

$$F(z,\omega) = \gamma\Big\{1 - \sigma(1 - \delta^2) + (\sigma/4)|Q|^2 a^4 z^{-4}\left[5\delta^4 - 2\delta^6 + z^2k^2(6\delta^2 - 5\delta^4)\right] + 2\sigma|Q|a|z|^{-1}\left[\delta(1 - \delta^2 - k^2z^2)\cos\Delta' - \delta^2 k|z|\sin\Delta'\right]\Big\} \quad (9)$$

where $\Delta' = k|z|/\delta - kz + \zeta$ and $\sigma = \pi a^2/L^2$. We ignored terms of order $(kz)^3$ and higher. The three terms in Eq. (9) have the same meaning as in Eq. (8). In its derivation, we set the upper integration limit to infinity ignoring possible interference effects between near fields of different MNPs. This is justified for dilute MNP dispersions, and in reality, the MNPs will be randomly dispersed averaging-out possible interferences.

We test Eq. (9) against accurate finite-difference time-domain (FDTD)[17,21] simulations for Au MNPs[17] of radius $a = 4$ nm inside a $n_h = 2$ host, which is approximate to most organic solar cells. A dilute suspension at $f = 2.7\%$ ($L = 21.5$ nm) is assumed. The FDTD grid resolution is set to 0.25 nm. Fig. 1(b) plots the AE on a plane through the MNP center ($z = 0$). We also plot the partial contributions of the near-field and of the incident/near-field cross term. The agreement is excellent. In Fig. 1(c), we plot the AE vs z at $\lambda = 610$ nm corresponding to the SPR and at $\lambda = 700$ nm. The excellent agreement proves that the point dipole approximation is an adequate tool for studying such systems.

Fig. 2(a) compares the AE of theory and FDTD for increasing filling ratios, on the $z = 0$ plane. Excellent agreement is also found here, except of a theoretical underestimation at the SPR peak at high filling ratios. The reason is that Eq. (9) does not account for cavity effects which lead to higher fields in the space between the MNP.[2] These are seen in the two figure insets which plot the total intensity at $z = 0$. Aside that, the overall agreement is impressive considering that at $f = 14\%$, the cell size $L = 12.5$ nm is comparable to the MNP diameter $2a = 8$ nm. We stress the crucial importance of Eqs. (5) and (6) rescalings, which account for red-shifting and broadening with increasing filling ratio, and for the proper available power level.

Next, we perform the vertical integration from $z = -\infty$ to $z = +\infty$. To normalize we divide by L. The incident/near-field cross term is integrated between $z = -L/2$ and $z = L/2$ to avoid divergences that appear at infinity.

$$F(\omega) \cong \gamma\Big\{1 - f + 2f|Q|^2(1 + a^2k^2) + 2f|Q| \times \left(\left[1 - (k^2/8)(a^2 + 3L^2)\right]\cos\zeta - (3kL/4)\sin\zeta\right)\Big\} \quad (10)$$

where we ignored terms of order $(ka)^3$, $(kL)^3$, and higher. For $a \ll \lambda$, this further simplifies to

$$F(\omega) \cong \gamma\{1 + f(2|Q|^2 + 2\mathrm{Re}\{Q\} - 1)\}. \quad (11)$$

Note that for $f \ll 1\%$, i.e., $L \gg a$, terms like $(kL)^3$ and higher must be included in Eq. (10). Such cases, however, are of no

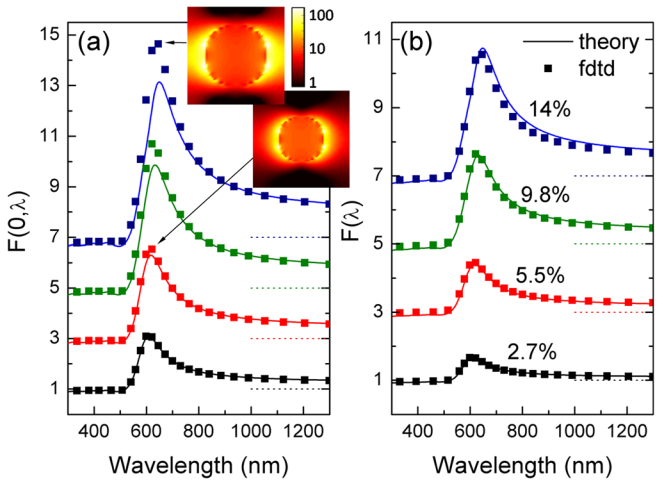

FIG. 2. (Color online) (a) Total enhancement vs wavelength on a plane through the Au MNP center, for four MNP arrays: $L=21.5$ nm ($f=2.7\%$), $L=17$ nm ($f=5.5\%$), $L=14$ nm ($f=9.8\%$) and $L=12.5$ nm ($f=14\%$). Lines for analytical and symbols for numerical results (vertically shifted by 2 for clarity). The insets plot the total intensity on a $z=0$ plane at $f=14\%$ and $f=5.5\%$. (b) Total enhancement vs wavelength over all volume for the arrays considered in (a).

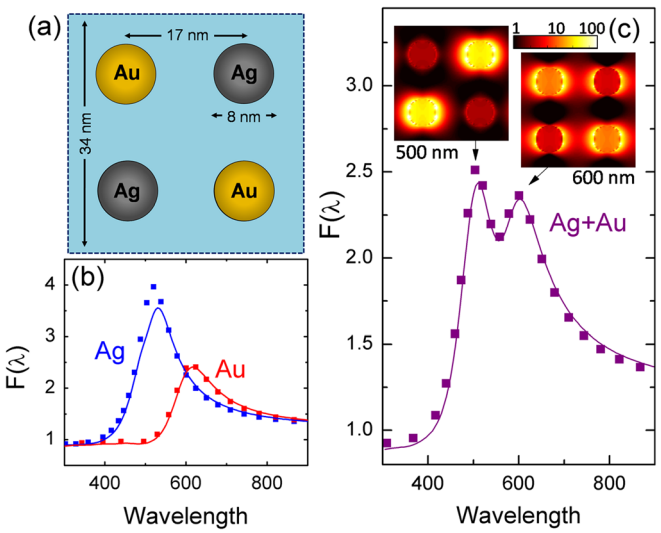

FIG. 3. (Color online) Schematic of a test case with mixed Au and Ag MNPs with $L=17$ nm ($f=5.5\%$). (b) Individual enhancement over all space of each MNP type at $f=5.5\%$ (c) Enhancement of the composite over all space. Lines for analytical and symbols for numerical results. The insets plot the field intensity at $\lambda=500$ nm (Ag SPR) and $\lambda=600$ nm (Au SPR).

practical interest. Eq. (10) is contrasted against FDTD in Fig. 2(b). Agreement is better than for the planar case due to volume averaging-out. Important AE is predicted below the SPR frequency, which for $f=14\%$ reaches above 70%.

Finally, we check on the predictive power of Eq. (10) on different MNP combinations. Fig. 3(a) shows the top view of a $f=5.5\%$ composite with Au and Ag (Ref. 22) MNPs. This is as the $f=5.5\%$ Au MNP case of Fig. 2, except that half of the Au MNPs are replaced by Ag MNPs. In such composites, the rescaling of Eq. (5) becomes $Q_i \to Q_i/(1-\sum f_i Q_i)$, where i runs through all MNP types and f_i is the corresponding partial volume filling ratio with $\sum f_i = f$. Also, the incident intensity rescaling of Eq. (6) becomes $\gamma = 1-(\sum f_i C_i)/(L^2 f)$, where L is the elementary unit cell for each MNP (in this case $L=17$ nm). All other terms in Eqs. (9)–(11) are just the corresponding weighted sums. The combined AE is shown in Fig. 3(c), while independent responses (one MNP type at $f=5.5\%$) are shown in Fig. 3(b). The insets plot the field intensity at $\lambda=500$ nm (Ag SPR) and $\lambda=600$ nm (Au SPR). The agreement between the theory and the FDTD is excellent, further validating the power of the dipole approximation. Moreover, the double peaks in Fig. 3(c) are a clear indication that using different MNP configurations, we can cover the whole visible and near IR spectrum, so to match the semiconductor's absorption spectrum and optimally enhanced its performance.

In conclusion, we derived analytical expressions for the surface plasmon near-field-mediated absorption enhancement expected for weakly absorbing organic semiconductors when doped with small metallic nanoparticles. Excellent agreement is found with accurate FDTD simulations, even in the case of mixed nanoparticle types, verifying our point dipole approximation. Our formulas provide an excellent tool for optimizing a nanoparticle dispersion to get enhanced absorption performance at particular points, planes, or volumes of the system. While we assumed a simplified geometry with no interfaces, and thus, no standing waves, we anticipate that such effects can be easily incorporated by appropriately rescaling the incident power. We are now working on exploring our formulas' validity and/or modifications for strongly absorbing semiconductors and realistic device geometries.

The authors acknowledge computing time at the Research Center for Scientific Simulations (RCSS) at the University of Ioannina.

[1]S. Gunes, H. Neugebauer, and N. S. Sariciftci, Chem. Rev. **107**, 1324 (2007).
[2]H. A. Atwater and A. Polman, Nature Mater. **9**, 205 (2010).
[3]D. Derkacs, S. H. Lim, P. Matheu, W. Mar, and E. T. Yu, Appl. Phys. Lett. **89**, 093103 (2006).
[4]S. Pillai, K. R. Catchpole, T. Trupke, and M. A. Green, J. Appl. Phys. **101**, 093105 (2007).
[5]K. Nakayama, K. Tanabe, and H. A. Atwater, Appl. Phys. Lett. **93**, 121904 (2008).
[6]A. J. Morfa and K. L. Rowlen, Appl. Phys. Lett. **92**, 013504 (2008).
[7]S.-S. Kim, S.-I. Na, J. Jo, D.-Y. Kim, and Y.-C. Nah, Appl. Phys. Lett. **93**, 073307 (2008).
[8]F.-C. Chen, J.-L. Wu, C.-L. Lee, Y. Hong, C.-H. Kup, and M. H. Huang, Appl. Phys. Lett. **95**, 013305 (2009).
[9]C. Min, J. Li, G. Veronis, J.-Y. Lee, S. Fan, and P. Peumans, Appl. Phys. Lett. **96**, 133302 (2010).
[10]V. E. Ferry, L. A. Sweatlock, D. Pacifici, and H. A. Atwater, Nano Lett. **8**, 4391 (2008).
[11]S. Pillai, F. J. Beck, K. R. Catchpole, Z. Ouyang, and M. A. Green, J. Appl. Phys. **109**, 073105 (2011).
[12]B. P. Rand, P. Peumans, and S. R. Forrest, J. Appl. Phys. **96**, 7519 (2004).
[13]H. Shen, P. Bienstman, and B. Maes, J. Appl. Phys. **106**, 073109 (2009).
[14]A. P. Kulkarni, K. M. Noone, K. Munechika, S. R. Guyer, and D. S. Ginger, Nano Lett. **10**, 1501 (2010).
[15]J. Zhu, M. Xue, H. Shen, Z. Wu, S. Kim, J.-J. Ho, A. Hassani-Afshar, B. Zeng, and K. L. Wang, Appl. Phys. Lett. **98**, 151110 (2011).
[16]J. B. Khurgin, G. Sun, and R. A. Soref, Appl. Phys. Lett. **94**, 071103 (2009).
[17]F. Schedin, E. Lidorikis, A. Lombardo, V. G. Kravets, A. K. Geim, A. N. Grigorenko, K. S. Novoselov, and A. C. Ferrari, ACS Nano **4**, 5617 (2010).
[18]C. F. Bohren and D. R. Huffman, *Absorption and Scattering of Light by Small Particles* (Wiley, New York, 1983).
[19]U. Kreibig and M. Vollmer, *Optical Properties of Metal Clusters* (Springer, Berlin, 1995).
[20]J. D. Jackson, *Classical Electrodynamics* (Wiley, New York, 1999).
[21]A. Taflove and S. C. Hagness, *Computational Electrodynamics: The Finite-Difference Time-Domain Method* (Artech House, Boston, 2005).
[22]E. D. Palik, *Handbook of Optical Constants of Solids* (Academic, San Diego, 1998).